Electronic Structure of Defect States in Hydroxylated and Reduced Rutile TiO$_2$(110) Surfaces

Cristiana Di Valentin and Gianfranco Pacchioni

Dipartimento di Scienza dei Materiali, Università di Milano-Bicocca, Via R. Cozzi 53, 20125 Milano, Italy

Annabella Selloni

Department of Chemistry, Princeton University, Princeton, New Jersey 08540, USA

It has been experimentally observed that a bridging oxygen vacancy on the rutile TiO$_2$(110) surface introduces localized Ti^{3+} $3d^1$ states about 1 eV below the conduction band which are not removed upon dissociation of a water molecule and formation of a pair of hydroxyl groups. Density functional calculations based on pure exchange-correlation functionals have not been able to satisfactorily reproduce and analyze these findings. Here we show that a correct description of the localized defect states on reduced and hydroxylated TiO$_2$(110) is achieved only if proper geometry relaxation is accounted for using hybrid exchange functionals. We confirm the electron trapping nature of Ti(OH) groups but find no evidence that these defects should also act as hole traps by formation of Ti^{4+}(OH)$^{\bullet}$ radicals.

Oxygen vacancies and hydroxyl groups are the two most common point defects on the surface of rutile TiO$_2$(110) and deeply affect the electronic properties and surface chemistry of this material [1]. The identification of these species has been the subject of an intense debate, and their role in surface processes has been sometimes confused, partly because freshly prepared reduced (O-deficient) TiO$_2$ surfaces quickly undergo hydroxylation even under UHV conditions. In fact, water readily dissociates on oxygen vacancies (O$_v$) to form pairs of nearby bridging hydroxyl (OH) groups [2]. This makes a clear distinction of O$_v$ and OH species challenging with many experimental techniques. For instance, electron energy loss (EELS) experiments [3] do not show significant changes of the O$_v$-induced electronic states on TiO$_2$(110) upon water adsorption, and also the interpretation of scanning tunneling microscopy (STM) images has been quite controversial [4–6]. On the other hand, signatures differentiating reduced and hydroxylated surface are clearly observed in ultraviolet photoemission spectroscopy (UPS) [7].

The role of O vacancies in surface processes, such as dissociation of organic molecules or stabilization of supported metal clusters, is well recognized [1]. Hydroxyls are active species in photocatalysis and photoinduced hydrophilicity [8,9], and Ti(OH) groups are supposed to be important surface traps for charge carriers, forming Ti^{4+}(OH)$^{\bullet}$ radicals (hole trapping) or Ti^{3+}(OH) groups (electron trapping) [8]. However, while the existence of photogenerated electrons giving rise to Ti^{3+} defect states was firmly established by electron paramagnetic resonance (EPR) [10,11], the role of Ti(OH) groups as hole traps is more controversial. For instance, recent experiments indicate that O$_2$ photoevolution is initiated by the attack of a H$_2$O molecule on a photogenerated hole at a surface lattice O site, not by a Ti^{4+}(OH)$^{\bullet}$ radical [12].

Theory is of key importance to unravel the electronic properties of different species. However, density functional theory (DFT) has well-known limitations in the description of localized states, particularly of excess electrons and holes in wide band-gap semiconductors and insulators. This is due to the insufficient cancellation of the self-interaction energy and the underestimation of the band gap (E_g). Use of Hartree-Fock or hybrid DFT methods, where the exact Fock exchange is partially mixed with the DFT exchange, significantly improves the description of trapped electron states [13–16]. In particular, the Becke 3-parameter Lee-Yang-Parr (B3LYP) functional [17], originally fitted to reproduce molecular properties, has proved to successfully overcome many of the problems encountered with the local-density approximation and the generalized gradient approximation in the solid state [18]; e.g., it improves E_g for many oxides [19]. So far, most of the theoretical studies dealing with reduced or hydroxylated TiO$_2$ surfaces have employed "pure" DFT approaches [20–24], thus suffering from the above mentioned limitations. Furthermore, while several DFT studies have dealt with either the energetics of H$_2$O dissociation at O$_v$ sites or the OH reactivity, the electronic structure of the hydroxylated surface has not been discussed yet [2,5]. A correct description of the electronic structure of hydroxylated TiO$_2$(110), and of its similarities and differences with that of the reduced surface, is crucial for understanding the surface reactivity and photochemistry of TiO$_2$. An accurate prediction of the electronic states of the defect species is also essential for the simulation of STM images.

In this work, we provide firm theoretical evidence that the O$_v$-induced defect states are not removed upon dissociation of a water molecule and formation of a pair of OH groups. Both defects give rise to localized Ti^{3+} $3d^1$ states about 1 eV below the conduction band (CB). Furthermore, for the first time we confirm the often invoked electron trapping nature of Ti(OH) groups, while we find no evidence that these species can also act as hole traps by formation of Ti^{4+}(OH)$^{\bullet}$ radicals. Our analysis is based

on DFT calculations using both pure and hybrid functionals. This allows us to show that pure DFT fails in describing defect states of reduced and hydroxylated $TiO_2(110)$ surfaces. Because of the strong (polaronlike) dependence on the local atomic structure, a correct description of these states is achieved only if geometry relaxation is accounted for with hybrid functionals.

The calculations have been performed within spin-polarized DFT, using both the hybrid B3LYP [17] and the gradient-corrected Perdew-Burke-Ernzerhof (PBE) [25] functionals. The Kohn-Sham orbitals were expanded in Gaussian-type orbitals, as implemented in the CRYSTAL03 code [26] [the all-electron basis sets are Ti 86411(d41), O 8411(d1), and H 311(p1)]. The reduced and hydroxylated $TiO_2(110)$ surfaces have been modeled by removing one oxygen and by adding two H atoms, respectively, to a clean periodic slab of four O-Ti-O trilayers [27,28]. A $c(4 \times 2)$ surface cell was used with the minimum distance between periodically repeated images of the defect of ≈ 9 Å. This corresponds to one O_v or a pair of OH groups every four bridging oxygens. The 2D Brillouin zone was sampled using 4 k points. Geometry optimizations were performed using the Berny algorithm, until the largest component of the ionic forces was less than 1×10^{-3} a.u., except for the atoms in the bottom layer which were fixed at their bulk positions. For comparison, PBE calculations have been carried out also using the PWSCF plane-wave pseudopotential code [29] (see Refs. [30,31] for details). The geometrical setup and k-space sampling was the same as for the CRYSTAL calculations, except for the PWSCF use of a periodically repeated slab geometry (vacuum of ≈ 10 Å between slabs). The agreement between the two sets of calculations was excellent.

On the reduced and hydroxylated surfaces, two excess electrons are present which originate from O removal (reduced surface) or from H addition. (While experimentally the hydroxylation results from dissociative H_2O adsorption at an O_v, formally it can be seen as the addition of two H atoms to the regular TiO_2 surface.) The two extra electrons can either be paired in a singlet closed shell state or form a paramagnetic triplet state. At the PBE level, the two configurations on the hydroxylated surface are almost degenerate. The states of the excess electrons are practically indistinguishable from CB states, as shown in Fig. 1 (PBE/PBE, left panel), and further evidenced by the delocalization over a large number of Ti atoms of either the spin density distribution (for the spin-polarized solution) or the charge density for the highest occupied level (for the closed shell solution). This result is due to the already mentioned tendency of DFT to underestimate E_g (2.1 eV for bulk rutile [31], against an experimental value of 3.0 eV [1]) and to delocalize trapped electrons so as to reduce self-interactions. Very similar considerations hold for the electronic structure of the system containing an isolated O_v,
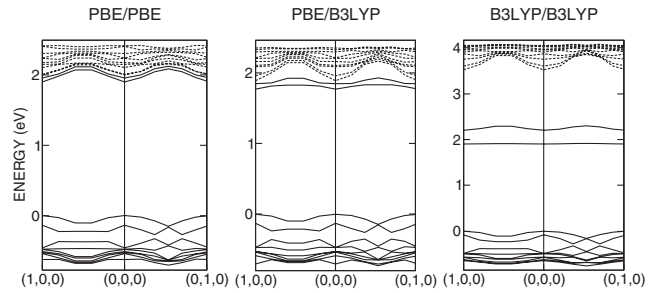

FIG. 1. Band structures for the hydroxylated $TiO_2(110)$ surface along the main symmetry directions of the surface Brillouin zone. Left panel: PBE energies with PBE optimized geometry (PBE/PBE); middle panel: PBE energies with B3LYP optimized geometry (PBE/B3LYP); right panel: B3LYP energies with B3LYP optimized geometry. Continuous (dashed) lines represent occupied (empty) states. Only the majority spin component is reported.

which gives rise to largely delocalized states, as reported previously [23,24]. In contrast with these theoretical results, however, experiments clearly show the occurrence of O_v-induced localized Ti^{3+} states [3,7,10]. Thus, pure DFT functionals do not account for this basic aspect of the electronic structure of the defect [27].

The B3LYP calculations provide a quite different picture. First, E_g for bulk rutile, 3.4 eV [19], is closer to experiment than the PBE value. Second, and more important, closed shell singlet and open shell triplet configurations for the hydroxylated surface converge to two different geometries, with the spin-polarized solution more stable by 0.6 eV. The energy gain of adsorbing a water molecule at O_v, 1.8 eV (B3LYP), is considerably larger than in PBE (0.94 and 0.97 eV according to Refs. [2,30], respectively), mainly because the triplet is definitely more stable. From the thermal programmed desorption peak at 520 K [3], a value of ~ 1.4 eV is estimated using Redhead's equation. Analysis of the energy levels for the hydroxylated surface shows two nearly flat bands in the gap, at about 1.6 and 1.2 eV below the bottom of the CB; see Fig. 1 (B3LYP/ B3LYP, right panel). The system is nonconducting, in contrast to the PBE result which gives the Fermi energy in the CB. The two bands in the gap correspond to two distinct peaks in the density of states (Fig. 2). The projections of these states on two specific Ti atoms almost fully account for the entire peak integral area. In fact, the spin density plots show that the excess electrons of the hydroxylated surface are trapped by two Ti ions which are reduced to Ti^{3+}. These two Ti ions are a sixfold coordinated Ti between the two bridging hydroxyls [d_{xz} state, 1.6 eV below the CB, hereafter referred to as Ti_{br-OH}^{3+}; Fig. 2(a)] and a nearby fivefold coordinated Ti [d_{xy} state, 1.2 eV below the CB, denoted as Ti_{5c}^{3+}; Fig. 2(b)]. For the singlet state, only one peak is present in the gap, 0.8 eV below the CB. Since the cost to reduce $Ti^{4+}(3d)^0$ to closed shell $Ti^{2+}(3d)^2$ is very high, the singlet coupling forces the
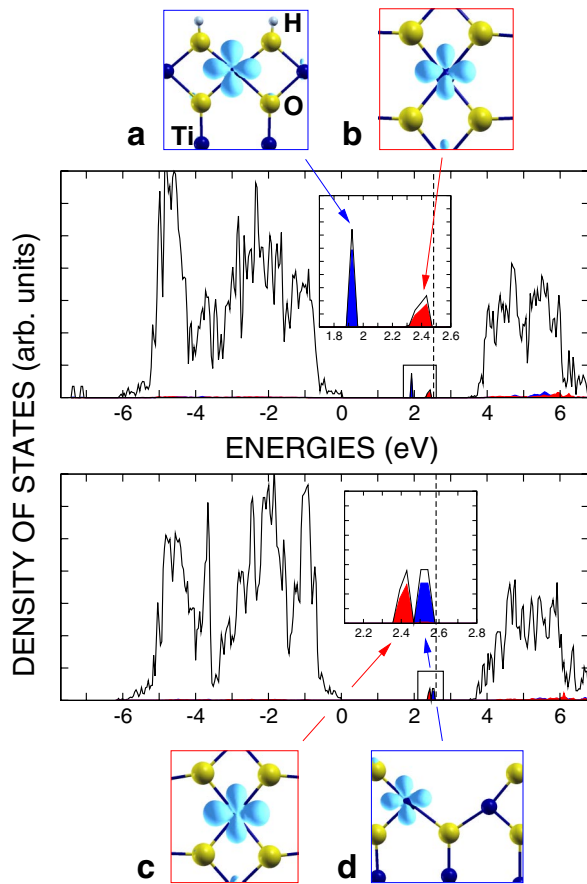
FIG. 2 (color online). Total and projected density of states for the hydroxylated (top) and reduced (bottom) $TiO_2(110)$ surface, calculated using the B3LYP hybrid functional. The Ti^{3+} states are localized on: (a) the Ti ion between the two bridging OH groups, Ti_{br-OH}^{3+}; (d) the Ti ion nearest to the oxygen vacancy, Ti_{br-v}^{3+}; (b),(c) on a five-coordinated Ti ion, Ti_{5c}^{3+}, of the surface. Spin density plots are reported: (a),(d) Ti_{br}^{3+}, side view; (b),(c) Ti_{5c}^{3+}, top view. The vertical dotted line in the PDOS denotes the position of the Fermi energy. Only the majority spin component is reported.

system to form a direct *d-d* bond between two adjacent $Ti^{3+}(3d)^1$ atoms which approach each other. This structure not only is less stable than the paramagnetic one but has never been observed, proving that spin polarization is essential to obtain a correct description of this system.

The electron trapping in Ti $3d$ states on the hydroxylated surface induces important structural distortions; see Fig. 3. Ti-O distances for the bridging oxygen of the clean surface are 1.82 Å; those of the Ti_{5c} rows are 1.95–1.96 Å. On the hydroxylated surface, the bond lengths around the defect are significantly elongated, and both Ti_{5c}^{3+} and Ti_{br-OH}^{3+} cations form Ti-O distances between 2.03 and 2.06 Å. Notice that the perturbation extends to the first and second neighbors, typical of a polaronic distortion.

The structural rearrangements found with the hybrid B3LYP functional are not observed in the PBE optimized
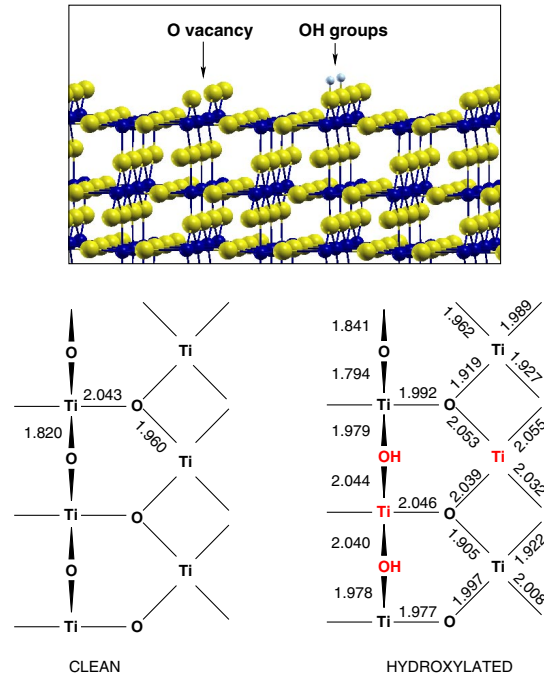

FIG. 3 (color online). Upper panel: Side view of $TiO_2(110)$ with one surface O vacancy and two surface OH groups (O atoms are large light spheres and Ti atoms are small dark spheres). Lower panel: Ti-O bond lengths (in Å) on the uppermost layer of the clean (left) and hydroxylated (right) $TiO_2(110)$ surfaces (top view).

geometry. According to the latter, on the hydroxylated and reduced surfaces there is only a modest elongation of the Ti-O distances of the bridging TiOH groups, as compared to the defect-free (110) surface. No change is found for the Ti_{5c}-O bond lengths, as no local electron trapping occurs with pure DFT. Clearly, structural relaxation plays a key role in the electron trapping phenomenon. To prove this, we performed a PBE calculation of the hydroxylated surface using the optimal B3LYP geometry. As shown by the band structure in Fig. 1 (PBE/B3LYP, middle panel), two well defined occupied Ti $3d$ states are now present just at the bottom of the CB. These states are localized on the Ti_{5c}^{3+} and Ti_{br-OH}^{3+} ions, and the charge density plots (not reported for brevity) show the same $3d$ character as in Figs. 2(a) and 2(b). Thus, the use of a properly distorted geometry is sufficient to achieve local electron trapping on atomic Ti $3d$ states even with the PBE functional. What remains to be clarified is whether with hybrid functionals electron localization can be obtained even without distortion of the atomic structure. To check this, we performed a B3LYP calculation on the PBE optimal geometry. The excess electrons are delocalized on several Ti atoms even at the B3LYP level, so that no distinct state appears in the projected density of states (PDOS) and in the band structure. Thus, proper structural relaxation is both a sufficient and a necessary condition to achieve a localized solution.

However, in order to obtain the correct structural distortion, some amount of exact exchange is needed.

There is another important feature in the PDOS of the hydroxylated TiO_2 rutile surface (top of Fig. 2). Two peaks below the O $2p$ valence band, at about -7 eV, are due to the two hydroxyl σ bonding O-H states (the antibonding counterparts lie very high in the CB). The remaining O $2p$ states of the OH groups, which are also stabilized with respect to those of the bridging oxygens, are spread within the O $2p$ band, giving very little contribution to the top of the band (a larger contribution to the latter comes from the neighboring surface oxygens). This suggests that the OH groups are not very efficient hole traps, as it has frequently proposed in the past [8]. On the contrary, the Ti atom of the TiOH group [in the configuration shown in Fig. 2(a)] is a good electron trap, as the corresponding energy level for Ti_{br-OH}^{3+} lies 1.6 eV below the CB. Of course, once the electron is trapped, $Ti^{3+}OH$ can attract and neutralize a hole, i.e., behave as a recombination center.

It is interesting to compare the structure of Ti(OH) to that of an isolated O_v. For the latter, the use of the hybrid B3LYP functional also leads to a localization of the excess electrons on two specific Ti atoms of the surface. Rather than trapping at the two undercoordinated Ti atoms nearest neighbors to the vacancy (Ti_{br-v}), one unpaired electron remains on a Ti_{br-v} ion and the other moves to a Ti_{5c} ion near O_v, probably to reduce electron repulsion. Thus, the two unpaired electrons are trapped on two *nonequivalent* Ti ions exactly as for the hydroxylated surface (Fig. 2). The PDOS (bottom of Fig. 2) shows that the two Ti^{3+} $3d$ states have a smaller energy separation and are closer to the bottom of the CB (1.1 and 0.9 eV) than on the hydroxylated surface (top of Fig. 2). Also, the order of the two states is reversed with respect to the OH species. The energies of these states are in very good agreement with EELS [3] and UPS [7] data. Furthermore, the EPR-measured g tensor of 1.96 for reduced TiO_2 is typical of localized $Ti^{3+}(3d^1)$ states [10,32], providing additional support to the picture given by the hybrid approach.

In conclusion, our results show that water dissociation at an oxygen vacancy does not remove the gap states associated with the vacancy nor change the orbital localization of these states, apart from a modest energy stabilization of the corresponding levels. In addition, our results show that the Ti(OH) defect can be a good electron trap, that the lattice distortion is essential in the electron trapping process, and that all of these effects can be properly described only using a spin-polarized approach where self-interactions are largely cancelled, as with a hybrid exchange functional (e.g., B3LYP). We believe that the present results will be valuable for the interpretation of the surface chemistry of rutile TiO_2.

[1] U. Diebold, Surf. Sci. Rep. **48**, 53 (2003).
[2] R. Schaub *et al.*, Phys. Rev. Lett. **87**, 266104 (2001).
[3] M. A. Henderson *et al.*, J. Phys. Chem. B **107**, 534 (2003).
[4] R. Schaub *et al.*, Science **299**, 377 (2003).
[5] S. Wendt *et al.*, Phys. Rev. Lett. **96**, 066107 (2006).
[6] D. Bicondoa *et al.*, Nat. Mater. **5**, 189 (2006).
[7] R. L. Kurtz, Surf. Sci. **218**, 178 (1989).
[8] M. R. Hoffmann *et al.*, Chem. Rev. **95**, 69 (1995).
[9] A. Fujishima, T. N. Rao, and D. A. Tryk, J. Photochem. Photobio. C **1**, 1 (2000).
[10] E. Serwicka, M. W. Schlierkamp, and R. N. Schindler, Z. Naturforsch. **36a**, 226 (1981).
[11] D. C. Hurum *et al.*, J. Phys. Chem. B **107**, 4545 (2003).
[12] R. Nakamura and Y. Nakato, J. Am. Chem. Soc. **126**, 1290 (2004).
[13] G. Pacchioni *et al.*, Phys. Rev. B **63**, 054102 (2001).
[14] W. C. Mackrodt, E.-A. Simson, and N. M. Harrison, Surf. Sci. **384**, 192 (1997).
[15] Y. Zhang *et al.*, J. Phys. Chem. B **109**, 19270 (2005).
[16] T. Bredow and G. Pacchioni, Chem. Phys. Lett. **355**, 417 (2002).
[17] A. D. Becke, J. Chem. Phys. **98**, 5648 (1993); C. Lee, W. Yang, and R. G. Parr, Phys. Rev. B **37**, 785 (1988).
[18] F. Cora' *et al.*, Structure and Bonding (Berlin) **113**, 171 (2004).
[19] J. Muscat, A. Wander, and N. M. Harrison, Chem. Phys. Lett. **342**, 397 (2001).
[20] M. Ramamoorthy, R. D. King-Smith, and D. Vanderbilt, Phys. Rev. B **49**, 7709 (1994).
[21] P. J. D. Lindan *et al.*, Phys. Rev. B **55**, 15919 (1997).
[22] A. T. Paxton and L. Thien-Nga, Phys. Rev. B **57**, 1579 (1998).
[23] M. D. Rasmussen, L. M. Molina, and B. Hammer, J. Chem. Phys. **120**, 988 (2004).
[24] Y. Wang, D. Pillay, and G. S. Hwang, Phys. Rev. B **70**, 193410 (2004).
[25] J. P. Perdew, K. Burke, and M. Ernzerhof, Phys. Rev. Lett. **77**, 3865 (1996).
[26] V. R. Saunders *et al.*, *CRYSTAL03 User's Manual* (University of Torino, Torino, 2003).
[27] Numerous tests were carried out to check that the conclusions of the present work do not depend on the number of layers. Details will be reported elsewhere.
[28] T. Bredow *et al.*, Phys. Rev. B **70**, 035419 (2004).
[29] S. Baroni *et al.*, http://www.pwscf.org.
[30] A. Tilocca, C. Di Valentin, and A. Selloni, J. Phys. Chem. B **109**, 20963 (2005).
[31] M. Lazzeri, A. Vittadini, and A. Selloni, Phys. Rev. B **63**, 155409 (2001).
[32] J. A. Weil, J. R. Bolton, and J. E. Wertz, *Electron Paramagnetic Resonance* (Wiley, New York, 1994).